Available online at www.sciencedirect.com
SCIENCE DIRECT®
Biochemical and Biophysical Research Communications 332 (2005) 181–187
BBRC
www.elsevier.com/locate/ybbrc

RIP3 β and RIP3 γ, two novel splice variants of receptor-interacting protein 3 (RIP3), downregulate RIP3-induced apoptosis

Yonghui Yang [a], Weiping Hu [b,1], Shanshan Feng [a], Jun Ma [a], Mian Wu [a,c,*]

[a] *Hefei National Laboratory for Physical Sciences at Microscale and School of Life Sciences, University of Science and Technology of China, Hefei, Anhui 230026, People's Republic of China*
[b] *Department of Obstetrics and Gynaecology, Singapore General Hospital, Singapore 169608, Singapore*
[c] *School of Biological Sciences, Nanyang Technological University, 60 Nanyang Drive, Singapore 637551, Singapore*

Received 19 April 2005
Available online 28 April 2005

Abstract

Receptor-interacting protein 3 (RIP3) is an apoptosis inducing member of the RIP family. Here we report two novel splice variants of human RIP3, designated RIP3 β and RIP3 γ respectively. Unlike full-length RIP3, both variants possess a truncated N-terminal kinase domain and a distinct and shorter C terminus, and therefore abrogate nucleocytoplasmic shuttling and apoptosis-inducing activity. Transient expression of either variant was found to downregulate RIP3-mediated apoptosis. Importantly, real-time PCR analysis reveals that the ratio of RIP3 γ to RIP3 is significantly increased in colon and lung cancers relative to their matched normal tissues, indicating that RIP3 γ might be a major splice form associated with tumorigenesis.

Keywords: RIP3; Splice variant; Apoptosis; Nucleocytoplasmic shuttling; Tumorigenesis

The receptor-interacting protein (RIP) family members are Ser/Thr kinases that are implicated in activation of NF-κB and induction of apoptosis [1]. Thus far, at least five RIP family members including RIP, RIP2, RIP3, RIP4, and RIP5 have been reported [1–3]. RIP3 is a potent apoptosis-inducing protein involved in the tumor necrosis factor receptor-1 (TNFR1) signaling pathway [1,4–6].

RIP3 contains an N-terminal kinase domain and a unique C-terminal domain. It has been shown that the N terminus of RIP3 is required for its kinase activity and autophosphorylation, whereas the C terminus is responsible for caspase activation and apoptosis induction [1,4–6]. Furthermore, RIP3 is recruited to the TNFR1 signaling complex through interaction with RIP via their RIP homotypic interaction motif (RHIM), and then promotes apoptosis by activating caspases and/or by inhibiting RIP- and TNFR1-induced NF-κB activation [1,7]. However, the exact role of RIP3 in NF-κB activation remains controversial and needs to be further clarified [8,9]. Recently, we have shown that RIP3 is a nucleocytoplasmic shuttling protein with nuclear export signal (NES) and nuclear localization signal (NLS) [10].

In this study, we have isolated two novel RIP3 splice variants, RIP3 β and RIP3 γ. In contrast to full-length RIP3, both variants abrogate nucleocytoplasmic shuttling and pro-apoptotic activity, but can downregulate RIP3-induced apoptosis. More importantly, RIP3 γ might function as a major splice form associated with tumorigenesis.

* Corresponding author. Fax: +86 551 3606264.
E-mail address: wumian88@yahoo.com (M. Wu).
[1] Present address: Genelabs Diagnostics Pte Ltd, 85 Science Park Drive #04-01, The Cavendish, Singapore 118259, Singapore.

0006-291X/$ - see front matter © 2005 Elsevier Inc. All rights reserved.
doi:10.1016/j.bbrc.2005.04.114

Materials and methods

Oligonucleotides and plasmid construction. Primers used for the PCR amplification of full-length RIP3 were: P1: 5′-GAAGATCT GTCGACATGTCGTGCGTCAAGTTATG-3′ and P2: 5′-CCGCTC GAGGCGGCCGCTTATTTCCCGCTATGATTAT-3′. The resulting PCR fragments encoding RIP3, RIP3 β, and RIP3 γ were digested with *Bgl*II/*Xho*I and then cloned into the *Bgl*II/*Sal*I sites of pEGFP-C1 (Clontech) to generate pEGFP-C1/RIP3, pEGFP-C1/RIP3 β, and pEGFP-C1/RIP3 γ. The cDNA sequences encoding RIP3, RIP3 β, and RIP3 γ were digested with *Sal*I/*Not*I and subcloned into the compatible sites of pCI-neo/Myc to create pCI-neo/Myc-RIP3, pCI-neo/Myc-RIP3 β, and pCI-neo/Myc-RIP3 γ. Primers used for the verification of splicing pattern were as follows: Psv-1: 5′-GAACT GTTTGTTAACGTAAA-3′, Psv-2: 5′-AAGCCGGGAGTCTCAGG CCC-3′, Psv-3: 5′-TGCTGGAAGAGAAGTTGAGT-3′, and Psv-4: 5′-AGGATCCCAGAATCCTCCTAGAGTCTT-3′.

Cell culture and transfection. HeLa cells were maintained in Dulbecco's modified Eagle's medium supplemented with 10% fetal bovine serum at 37 °C in 5% CO_2. Transfections were performed using LipofectAMINE 2000 (Invitrogen) according to the manufacturer's specifications.

Reagents and immunoblotting. Hoechst 33342, human recombinant TNF-α, and cycloheximide (CHX) were purchased from Sigma. Immunoblotting analysis was performed as previously described [10].

Real-time PCR. Total RNAs from different normal human tissues (Clontech) or human normal and matched tumor cDNA libraries (Clontech) were employed as template. Three gene-specific forward primers were: RIP3 (F): 5′-TGCTGGAAGAGAAGTTGAGTTGC-3′, RIP3 β (F): 5′-AGTGCTTGCTGGAAGAGAATGC-3′, and RIP3 γ (F): 5′-GGGATCCTTAACCCCAGTGC-3′. A common reverse primer (RIP3R, 5′-CTGTTGCACACTGCTTCGTACAC-3′) was used for all three RIP3 transcripts. Amplification was done by an initial incubation at 95 °C for 10 min, followed by 45 cycles of 95 °C for 15 sec, and 60 °C for 1 min. Real-time PCR was performed in an ABI Prism 7700 System according to the protocol suggested by the User Bulletin #2 (Applied Biosystems).

Flow cytometry. Apoptosis was assessed using a FACSCalibur flow cytometer and the CellQuest software (Becton–Dickinson) as described previously [11].

Results

Cloning of two novel splice variants of RIP3

To isolate the full-length human RIP3 gene, a single 1.5-kb fragment was amplified from a lymph node cDNA library (Clontech) and inserted into pEGFP-C1 vector. Unexpectedly, Western blot revealed that two independent clones expressed a protein with molecular weight (MW) of 28 kDa, which was much smaller than the expected 57 kDa, the predicted MW of full-length RIP3 protein (Fig. 1, lane 3). A HeLa cDNA library (Clontech) was next screened, and Western blot showed that while one in four independent clones expressed a 28 kDa protein, the remaining three expressed proteins of 25 kDa (Fig. 1, lane 4). Two additional results showed that all four clones isolated from Jurkat cells by RT-PCR gave rise to a 28 kDa protein; whereas all four independent clones isolated from a brain cDNA library (Clontech) expressed a protein with MW of

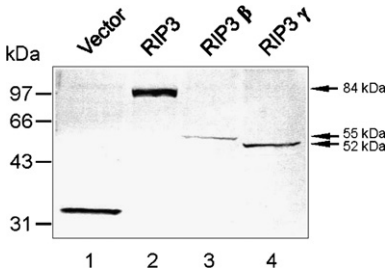

Fig. 1. Isolation of two novel RIP3 isoforms. HeLa cells were transfected with pEGFP-C1 control (lane 1), GFP-tagged RIP3 (lane 2), RIP3 β (lane 3), and RIP3 γ (lane 4), respectively. After 24 h, cell lysates were harvested and subjected to Western blotting using anti-GFP antibody.

57 kDa (Fig. 1, lane 2). Computational sequence analysis using BLAST revealed that the cDNA encoding the 57 kDa protein was identical to the full-length RIP3 gene, whereas the cDNAs encoding 28 and 25 kDa proteins turned out to be two novel RIP3 splice variants, which were then designated as RIP3 β and RIP3 γ, respectively. Nucleotide sequences coding for RIP3, RIP3 β, and RIP3 γ have been deposited in GenBank Accession Nos. AY453693, AY494982, and AY494983.

RIP3 β and RIP3 γ are generated through alternative splicing

To define the intron–exon organization of the RIP3 gene, BLAST searches of the human genome in the GenBank database revealed a BAC clone (RPCI11-934B9) from chromosome 14 (GenBank Accession No. AL096870), which contains the entire RIP3 gene. The human RIP3 gene contains 10 exons, spanning approximately 3.7 kb in size (Fig. 2A). Sequence analysis demonstrated that all the intron–exon junction sequences match the so-called GT-AG rule (data not shown).

Careful inspection of the RIP3 β and RIP3 γ coding sequences with the genomic sequences revealed the presence of two other cryptic splice donor (SD) sites, one is GAAGTTGAG (SD site II) near the 3′-end of exon 5, and the other is CAGGTGCCC (SD site III) within intron 5 (Fig. 2B). The canonical SD site I (AGTGTAA GA) and corresponding splice acceptor (SA) site (CCTCCCCTACTCCAGT) at the boundaries between intron 5 and exon 6 are normally utilized by RIP3 to yield a 1554 bp open reading frame (ORF) (Fig. 2B). By alternative mRNA splicing, the same SA site as for RIP3 was used, but RIP3 β was generated at SD site II with a 7 bp deletion from exon 5, resulting in a frame-shifted ORF of 756 bp, while RIP3 γ was produced at SD site III with a 38 bp insertion to be part of exon 5, leading to an altered reading frame with a 693 bp ORF (Figs. 2A and B).

The proposed splicing pattern was further verified by PCR analysis (Fig. 2C). Psv-1 and Psv-2 correspond to the position of 100 bp upstream and downstream of

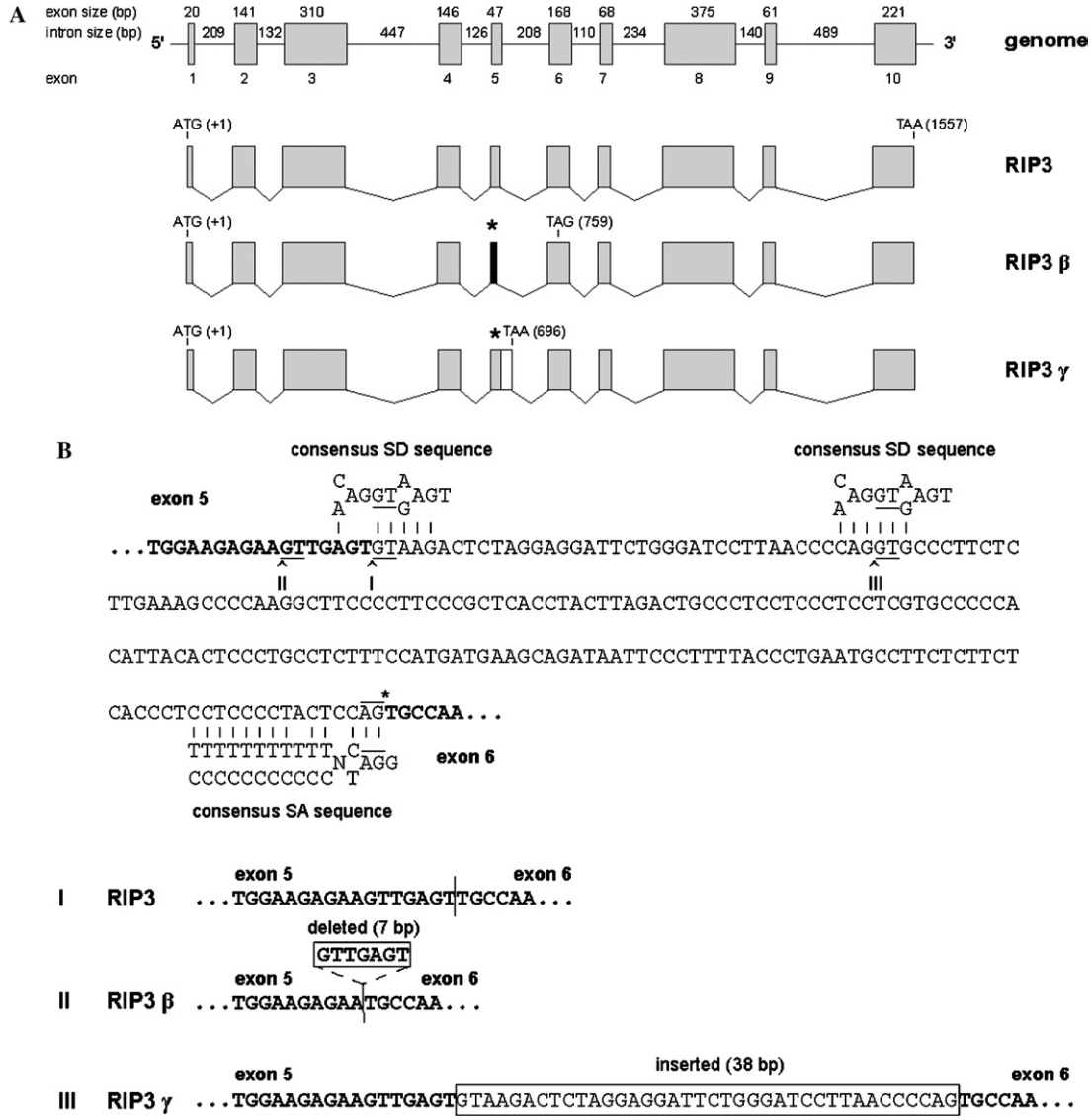

Fig. 2. RIP3 β and RIP3 γ are produced by alternative pre-mRNA splicing. (A) Organization of the RIP3 and its splice variant genes. Exons are represented as gray boxes, introns as thin line. The size of exon or intron is indicated and the number of exon is denoted. Asterisks represent alternatively spliced sites. The black box indicates exon 5 with deletion, and the open box indicates the insertion in exon 5. The positions of the start and termination codons are indicated. (B) The proposed splicing mechanism for RIP3, RIP3 β, and RIP3 γ. Nucleotides of exons 5 and 6 are shown in bold, and the sequence between exons 5 and 6 indicates intron 5. The consensus sequences for SD and SA sites are compared with the potential SD and SA sites in RIP3. The underlined GT marked with I, II, and III denotes 5′-SD site, and the overlined AG marked with an asterisk indicates 3′-SA site. The deleted 7 bp in RIP3 β and the inserted 38 bp in RIP3 γ are boxed. (C) Verification of alternative splicing pattern of the RIP3 and its variant genes by PCR analysis. The open blocks represent the exons flanking intron 5, the gray block indicates the deletion, and the black block denotes the insertion. Arrows represent the positions and orientations of the primers.

the exon 5/intron 5 junction, respectively, Psv-3 corresponds to the last 7 bp in exon 5 and Psv-4 to the first 38 bp in intron 5. PCR fragments of different sizes were amplified from RIP3 and its two variants using primer pair Psv-1/Psv-2. With primer pair Psv-3/Psv-2, fragments can be amplified from RIP3 and RIP3 γ, respectively, but no fragment can be amplified from RIP3 β due to a 7 bp deletion in its exon 5. Primer pair Psv-1/Psv-4 only amplified a 129 bp fragment from RIP3 γ, but not from RIP3 and RIP3 β in which intron 5 was completely spliced out.

Because of a reading frame shift and consequent premature stop codon, RIP3 β and RIP3 γ were produced as truncated proteins, and the first 219 residues in RIP3 β and RIP3 γ were identical to RIP3 and then diverged thereafter (Fig. 3).

Tissue distribution of RIP3, RIP3 β, and RIP3 γ

To investigate the expression pattern of RIP3 and its splice variants, real-time RT-PCR was performed (Fig. 4A). RIP3 γ was widely expressed at a comparable

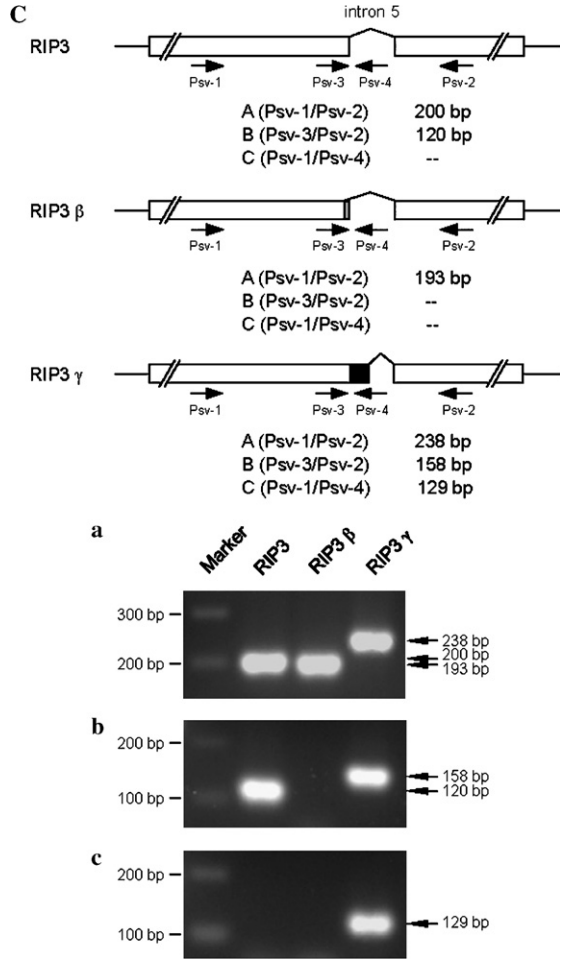

Fig 2. (*continued*)

level to RIP3 in the majority of tissues examined. Interestingly, however, little expression of RIP3 β can be detected, which is likely associated with the fact that SD site II does not match the consensus SD sequence well (Fig. 2B). Thus, we postulate that RIP3 γ might be the major splice form or the expression of RIP3 β is usually off in the normal tissues. Next, we employed real-time PCR to further explore the differential expression profiles of RIP3 and RIP3 γ in tumors and matched normal tissues (Fig. 4B). The ratio of RIP3 γ to RIP3 was found to be significantly increased in both colon and lung tumors relative to their matched normal tissues, implying that RIP3 γ might be involved in the tumorigenesis of some types of human cancer such as colon and lung cancers.

RIP3 β and RIP3 γ fail to shuttle between nucleus and cytoplasm

The possibility of RIP3 variants to traffic between nucleus and cytoplasm was assessed (Fig. 5). In contrast to our previous observation for GFP-RIP3 [10], GFP-RIP3 β was always detected in the cytoplasm in the presence or absence of LMB (a specific inhibitor of CRM1-dependent nuclear export), and a similar result was also obtained for RIP3 γ.

RIP3 β and RIP3 γ are unable to induce apoptosis

The apoptotic activity of splice variants was determined using flow cytometry (Fig. 6). Twenty-eight

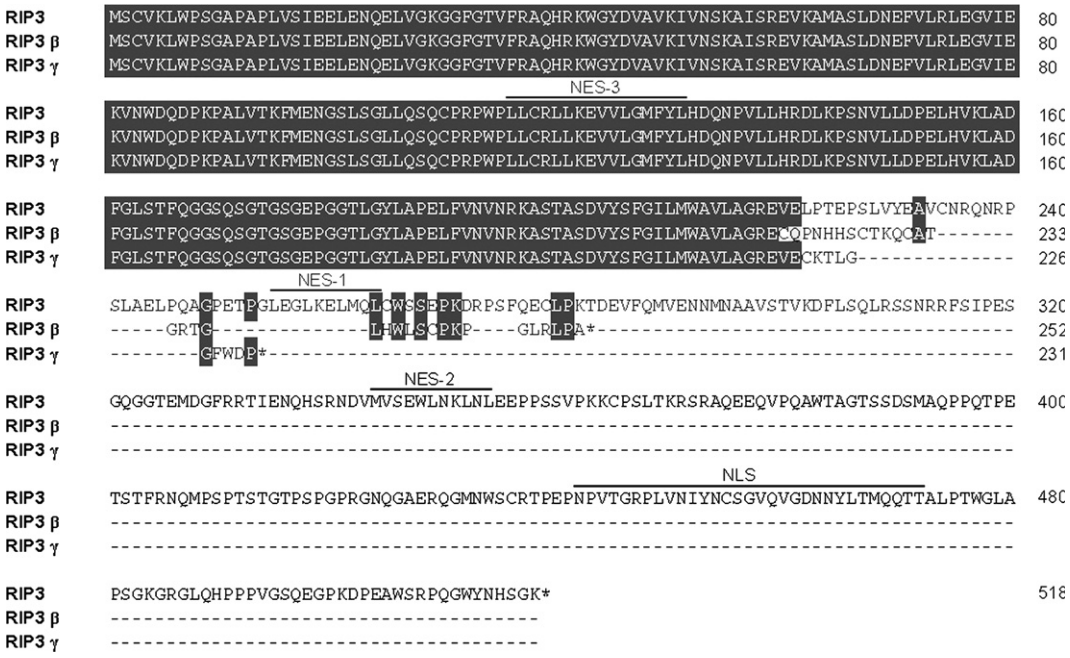

Fig. 3. RIP3 β and RIP3 γ are structurally distinct from RIP3. Multiple sequence alignments were performed using Multalin software [12]. Identical and similar residues are shown in black and gray shadings, respectively. The putative NESs and NLS are overlined and indicated. Asterisks denote the end of coding regions.

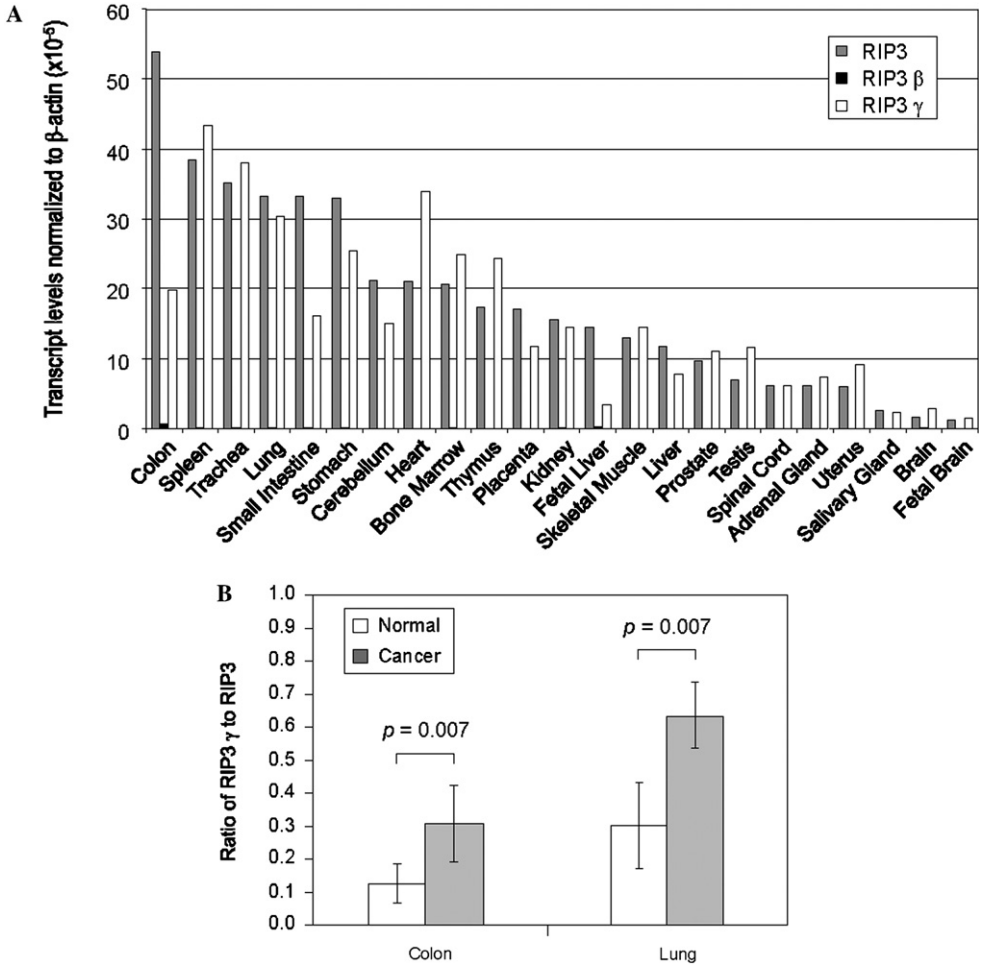

Fig. 4. Expression profiles of RIP3 and its splice variants in human tissues. (A) The distribution of RIP3 and its splice variants in 23 different normal human tissues was determined using real-time RT-PCR. All the transcript levels were normalized to β-actin. Data shown are means of triplicate independent experiments. (B) Differential expression pattern of RIP3 and RIP3 γ was analyzed by real-time PCR in human tumors and matched normal tissues. The ratio of RIP3 γ to RIP3 in each type of tissue sample ($n = 5$) was plotted as the mean ± SD. Paired t test was used to compare the ratio of RIP3 γ to RIP3 in the matched tissue samples.

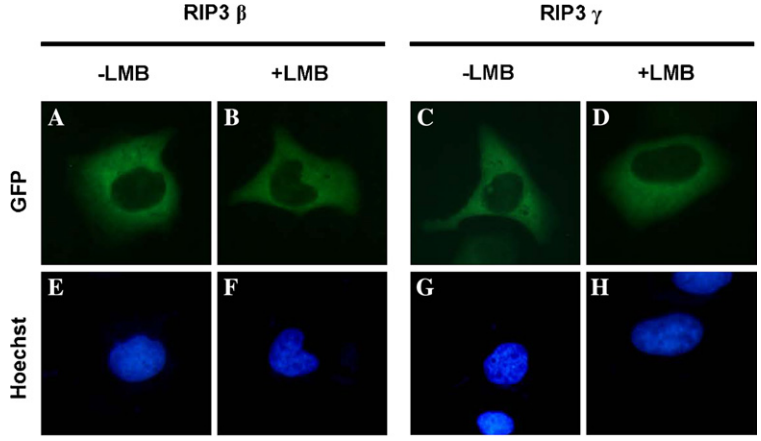

Fig. 5. RIP3 β and RIP3 γ are unable to shuttle between cytoplasm and nucleus. HeLa cells were transiently transfected with GFP-tagged RIP3 β (left panel) and RIP3 γ (right panel). After 24 h, HeLa cells were left untreated (A,C) or treated (B,D) with LMB (2 ng/ml) at 37 °C for 1 h, counterstained with Hoechst 33342 (E,G) or (F,H) respectively, and then examined by fluorescence microscopy (magnification, 400×).

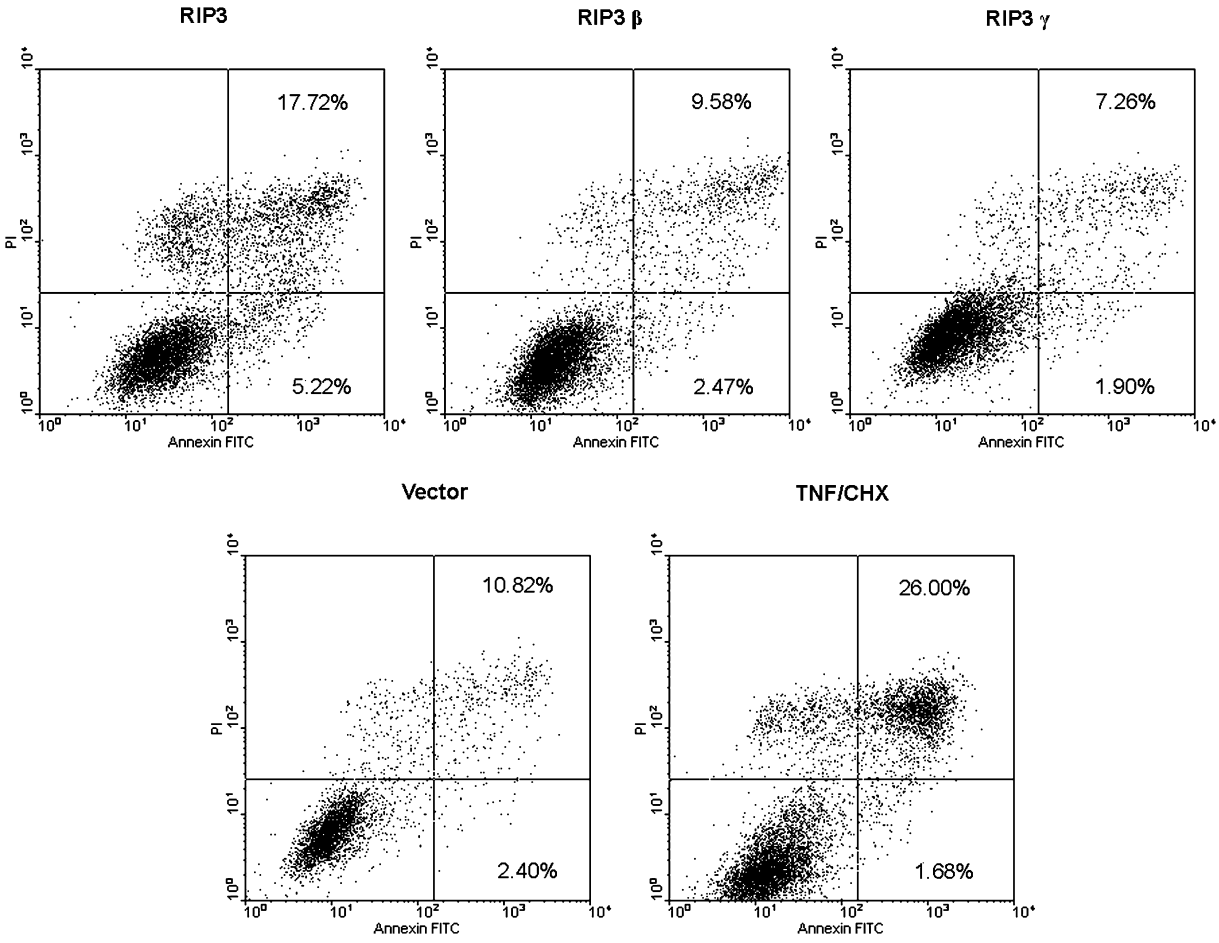

Fig. 6. RIP3 β and RIP3 γ abrogate their pro-apoptotic activity. HeLa cells were transfected with 0.5 μg pCI-neo (Promega) control, Myc-tagged RIP3, RIP3 β, and RIP3 γ for 24 h or treated only with TNF (2000 U/ml)/CHX (10 μg/ml) for 10 h, all cells were harvested for flow cytometry analysis.

percent and twenty-three percent cell death induced, respectively, by TNF/CHX and RIP3 were found to be significantly higher than the cell death induced by RIP3 β (12%) and RIP3 γ (9%), which were similar to 13% cell death caused by empty vector, suggesting that both RIP3 β and RIP3 γ have completely abolished their pro-apoptotic activity.

RIP3 β and RIP3 γ can downregulate RIP3-induced apoptosis

We have observed that overexpression of truncated C-terminal RIP3 reproducibly induced a more potent apoptosis than full-length RIP3, indicating that the N terminus of RIP3 might negatively regulate RIP3-induced apoptosis. Since RIP3 β and RIP3 γ contained the majority of N-terminal RIP3, it prompted us to consider the possibility that two RIP3 variants serve to down-regulate RIP3 itself. As shown in Fig. 7, transient over-expression of either RIP3 β or RIP3 γ can partially inhibit RIP3-induced apoptosis as an approximately 0.5-fold higher than control.

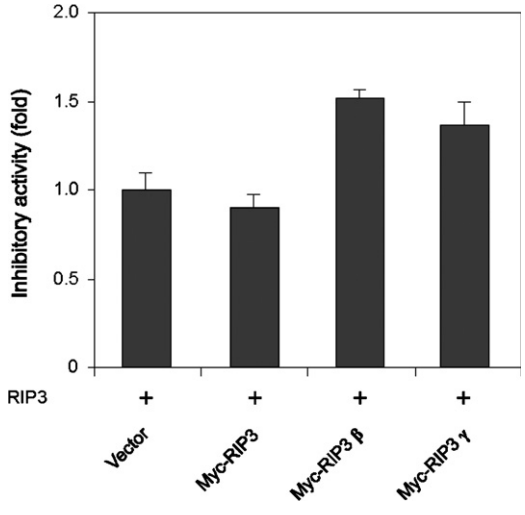

Fig. 7. RIP3 β and RIP3 γ suppress RIP3-induced apoptosis. HeLa cells were transiently cotransfected with pEGFP-C1/RIP3 (0.1 μg) together with pCI-neo empty vector or plasmids expressing Myc-tagged RIP3, RIP3 β or RIP3 γ (3 μg). After 20 h, apoptosis assays were performed mainly as described previously [10]. Data (means ± SD, $n = 3$) are shown as fold inhibition of apoptotic activity.

Discussion

In this study, we have identified two novel RIP3 variants, termed RIP3 β and RIP3 γ, which are produced by an alternative splicing mechanism. We have previously shown that RIP3 is a potent inducer of apoptosis with its activity localizable to amino acids 442–472, which happens to contain the core 16 residues of RHIM that is critical for the association with the RHIM of RIP and Trif [7,9,10]. Missing the functionally important C terminus, RIP3 β and RIP3 γ display neither pro-apoptotic activity nor inhibitory effect on TNF-induced apoptosis (data not shown). Significantly, however, RIP3 β and RIP3 γ are found to negatively regulate RIP3-induced apoptosis. In addition, both variants contain only the first nine but not the complete eleven kinase subdomains in RIP3, they presumably lack the kinase activity because the entire subdomains are essential for enzymatic activity [2].

Nucleocytoplasmic shuttling of RIP3 is believed to be critical for its function since the functions of many tumor suppressors including p53 and APC are regulated by their nucleocytoplasmic shuttling activity [13]. Comparatively, however, RIP3 β and RIP3 γ are localized to the cytoplasm and completely abolish nucleocytoplasmic shuttling ability.

Importantly, we have found that the ratio of RIP3 γ to RIP3 is significantly increased in at least colon and lung cancers relative to their matched normal tissues. At present, we do not have more evidences to claim that RIP3 γ is responsible for the tumorigenesis of colon or lung, nevertheless, loss of pro-apoptotic function of RIP3 γ is likely associated with cancer development.

The RIP3 gene is located on chromosome 14q11. 2, a locus frequently altered in many types of cancer including nasopharyngeal carcinoma and T-cell leukemia/lymphoma [6]. RIP3 induces extensive apoptosis, whereas RIP3 β and RIP3 γ have lost their pro-apoptotic function. Therefore, we propose that RIP3 might be a tumor suppressor. In support of this hypothesis, similar conclusions are drawn from Bim and Bcl-G, which have recently been ascribed to putative tumor suppressors [14,15].

We believe that RIP3 β and RIP3 γ are the first splicing variants identified in RIP family members since no splice variants have previously been reported. Although the identification of RIP3 splice variants considerably adds to the complexity of RIP3 functions, it will have important implications for our better understanding of the physiological roles of RIP3 and its splice variants.

Acknowledgments

We thank Dr. Minoru Yoshida for LMB and Dr. Ke Shuai for helpful discussions. This research was supported by a 973 Grant (2002CB713702) from the Ministry of Science and Technology of China, by grants from the National Natural Science Foundation of China (30370308, 90208027, and 30121001), by a grant from the Natural Science Foundation of Anhui Province (050430202), and by a Grant (SBS/SUG/22/04) to W.M. from Nanyang Technological University, School of Biological Sciences, Singapore.

References

[1] X. Sun, J. Lee, T. Navas, D.T. Baldwin, T.A. Stewart, V.M. Dixit, RIP3, a novel apoptosis-inducing kinase, J. Biol. Chem. 274 (1999) 16871–16875.
[2] E. Meylan, F. Martinon, M. Thome, M. Gschwendt, J. Tschopp, RIP4 (DIK/PKK), a novel member of the RIP kinase family, activates NF-κB and is processed during apoptosis, EMBO Rep. 3 (2002) 1201–1208.
[3] J. Zha, Q. Zhou, L.G. Xu, D. Chen, L. Li, Z. Zhai, H.B. Shu, RIP5 is RIP-homologous inducer of cell death, Biochem. Biophys. Res. Commun. 319 (2004) 298–303.
[4] P.W. Yu, B.C.B. Huang, M. Shen, J. Quast, E. Chan, X. Xu, G.P. Nolan, D.G. Payan, Y. Luo, Identification of RIP3, a RIP-like kinase that activates apoptosis and NF-κB, Curr. Biol. 9 (1999) 539–542.
[5] N.J. Pazdernik, D.B. Donner, M.G. Goebl, M.A. Harrington, Mouse receptor interacting protein 3 does not contain a caspase-recruiting or a death domain but induces apoptosis and activates NF-κB, Mol. Cell. Biol. 19 (1999) 6500–6508.
[6] G.M. Kasof, J.C. Prosser, D. Liu, M.V. Lorenzi, B.C. Gomes, The RIP-like kinase, RIP3, induces apoptosis and NF-κB nuclear translocation and localizes to mitochondria, FEBS Lett. 473 (2000) 285–291.
[7] X. Sun, J. Yin, M.A. Starovasnik, W.J. Fairbrother, V.M. Dixit, Identification of a novel homotypic interaction motif required for the phosphorylation of receptor-interacting protein (RIP) by RIP3, J. Biol. Chem. 277 (2002) 9505–9511.
[8] K. Newton, X. Sun, V.M. Dixit, Kinase RIP3 is dispensable for normal NF-κBs, signaling by the B-cell and T-cell receptors, tumor necrosis factor receptor 1, and Toll-like receptor 2 and 4, Mol. Cell. Biol. 24 (2004) 1464–1469.
[9] E. Meylan, K. Burns, K. Hofmann, V. Blancheteau, F. Martinon, M. Kelliher, J. Tschopp, RIP1 is an essential mediator of Toll-like receptor 3-induced NF-κB activation, Nat. Immunol. 5 (2004) 503–507.
[10] Y. Yang, J. Ma, Y. Chen, M. Wu, Nucleocytoplasmic shuttling of receptor-interacting protein 3 (RIP3): identification of novel nuclear export and import signals in RIP3, J. Biol. Chem. 279 (2004) 38820–38829.
[11] L. Miao, P. Yi, Y. Wang, M. Wu, Etoposide upregulates Bax-enhancing tumour necrosis factor-related apoptosis inducing ligand-mediated apoptosis in the human hepatocellular carcinoma cell line QGY-7703, Eur. J. Biochem. 270 (2003) 2721–2731.
[12] F. Corpet, Multiple sequence alignment with hierarchical clustering, Nucleic Acids Res. 16 (1988) 10881–10890.
[13] M. Fabbro, B.R. Henderson, Regulation of tumor suppressor by nuclear-cytoplasmic shuttling, Exp. Cell Res. 282 (2003) 59–69.
[14] S. Cory, D.C. Huang, J.M. Adams, The Bcl-2 family: roles in cell survival and oncogenesis, Oncogene 22 (2003) 8590–8607.
[15] A. Montpetit, G. Boily, D. Sinnett, A detailed transcriptional map of the chromosome 12p12 tumour suppressor locus, Eur. J. Hum. Genet. 10 (2002) 62–71.